*Elektrotehniški vestnik 70(4): 190–195, 2003*
*Electrotechnical Review, Ljubljana, Slovenija*

# Impact of magnetic saturation on the steady-state operation of the controlled induction motor

**Petar Ljušev, Drago Dolinar, Gorazd Štumberger**

*University of Maribor, Faculty of electrical engineering and computer science, Smetanova 17, Maribor, Slovenija*
*E-mail: pl@eltek.dtu.dk, dolinar@uni-mb.si*

**Abstract.** The paper presents a method for determination of the steady-state torque characteristics of the induction motor in the case of rotor field-oriented control (RFOC) with nonlinear magnetizing characteristic of the iron core included. The torque characteristics are determined for the constant stator current and the constant d-axis stator current. The characteristics obtained at a constant stator current are used to maximize the torque capability of the RFOC induction motor. The aim of the presented work is to obtain required steady-state torque with minimal stator current. Experiments show that the proposed selection of a magnetizing reference is promising.

**Key words:** induction motor, torque characteristics, magnetic saturation

# Vpliv magnetnega nasičenja na stacionarne obratovalne lastnosti reguliranega asinhronskega motorja

**Povzetek.** V članku je predstavljen postopek za določanje navornih karakteristik pri stacionarnem obratovanju asinhronskega stroja v orientaciji rotorskega polja z upoštevanjem magnetnega nasičenja železa. Določene so navorne karakteristike pri konstantnem statorskem toku $I_{sd}$ v d- osi (enačba (6) in sliki 1 in 2), izpostavljena pa je potreba upoštevanja nasičenja pri določitvi navornih karakteristik pri konstantnem statorskem toku $I_s$ z enačbo (7) (sliki 3 in 4). Določeni sta tudi krivulji maksimalnega navora v primeru vodenja asinhronskega stroja brez (9) in z (10) upoštevanjem nasičenja. Predlagan je algoritem za primeren izbor referenčne vrednosti toka $I_{sd}$, ki naj bi omogočal tvorjenje zahtevanega navora z najmanjšim statorskim tokom (enačbi (13) in (14)). Krivulja maksimalnega navora reguliranega asinhronskega stroja z upoštevanjem nasičenja je bila potrjena tudi eksperimentalno (sliki 6 in 7). Podani rezultati kažejo, da je smiselno spreminjati referenčno vrednost toka $I_{sd,ref}$ na predlagani način, saj s tem zagotovimo manjši statorski tok in manjše izgube.

**Ključne besede:** asinhronski stroj, navorne karakteristike, magnetno nasičenje

## 1 Introduction

Modelling of electrical machines is usually carried out with assumption of linear magnetic conditions and irrespective of the iron core magnetic saturation. The latter is accounted for only when modelling of induction motor is carried out for the purpose of control design. Exceptions can be found in [1], [2], [3], [4] where authors developed complex dynamic models of a saturated induction motor, with no intention to use them in a further control synthesis. Pioneering efforts to include magnetic saturation in control algorithms are found in literature [5], [6], [7]. The adverse effects of magnetic saturation on the field-oriented induction motor drives and especially their torque production are addressed in [8], [9], [10].

Operation of the induction motor drive strongly depends on a proper selection of the rotor flux linkage reference value which represents an additional degree of freedom in control design. Therefore, it can be used to optimize some of the drive features subjected to the voltage and current constraints. Authors in [6], [11], [12] investigate optimization of the induction motor torque in the region with or without field-weakening. Another approach [13] deals with the reference selection in order to reduce the motor active losses.

This paper is limited to the analysis of the steady-state operation of the RFOC induction motor with the rotor speed smaller than the base speed. Therefore, the voltage limitations are neglected and only the current limitation $I_{sd}^2 + I_{sq}^2 \leq I_{smax}^2$ is considered. At the same time, as frequently found in the literature, only magnetic saturation of the mutual inductance is taken into account. Using the equations of the induction motor in the RFOC torque characteristics of the induction motor with constant d-axis stator current $I_{sd}$ and constant stator current $I_s$ are developed. The obtained characteristics are used for determination of magnetizing current $I_{sd}$ which gives the maximal torque-stator current ratio. The curve of the maximal torque, including magnetic saturation which determines the ratio between the d-axis and the q-axis current for the

*Received 12 December 2002*
*Accepted 10 March 2003*

peak torque-per-ampere operation, is analytically determined.

Correctness of the described analytical method and feasibility of the proposed d-axis stator current reference selection are proven experimentally.

In section 2, an induction motor model in the rotor field-oriented reference frame is presented. In section 3, the torque characteristics of the controlled induction motor with $I_{sd} = const.$ and $I_s = const.$ are determined as a function of the ratio $I_{sq}/I_s$ with and without taking into account magnetic saturation. Differences between the characteristics are emphasized as they give rise to further differences when choosing an appropriate magnetizing reference in the form of the d-axis stator current $I_{sd}$ reference. The algorithm for the varying d-axis stator current $I_{sd}$ reference in order to achieve the required torque with minimal stator current $I_s$ is presented in section 4. Simulation and experimental results are presented in section 5. In section 6 some concluding remarks are made.

## 2 A saturated induction motor model in RFOC

A saturated induction machine model is developed in the same way as in [1]. In the case of rotor field-oriented reference frame ($\psi_{rq} = 0$) the dynamic induction motor model has the following form:

$$\begin{aligned} u_{sd} &= R_s i_{sd} + \tfrac{d\psi_{sd}}{dt} - \omega_{mr}\psi_{sq} \\ u_{sq} &= R_s i_{sq} + \tfrac{d\psi_{sq}}{dt} + \omega_{mr}\psi_{sd} \\ u_{rd} &= R_r i_{rd} + \tfrac{d\psi_{rd}}{dt} = 0 \\ u_{rq} &= R_r i_{rq} + (\omega_{mr} - \omega_r)\psi_{rd} = 0 \\ t_e &= pL_m(i_{sq}i_{rd} - i_{sd}i_{rq}) = p\tfrac{L_m}{L_r}\psi_{rd}i_{sq} \\ J\tfrac{d\omega_r}{dt} &= t_e - t_l - f\omega_r \end{aligned} \tag{1}$$

where $u_{sd}$ and $u_{sq}$ are the stator voltages, $u_{rd}$ and $u_{rq}$ are the rotor voltages, $i_{sd}$ and $i_{sq}$ are the d-axis and the q-axis stator currents, $i_{rd}$ and $i_{rq}$ are the d-axis and the q-axis rotor currents, $\psi_{sd}$ and $\psi_{sq}$ are the stator flux linkages, $\psi_{rd}$ and $\psi_{rq}$ are the rotor flux linkages, $R_s$ and $R_r$ are the stator and the rotor resistance, $L_m = \Psi_m/i_m$ is the mutual static inductance, $L = d\Psi_m/di_m$ is the mutual dynamic inductance, $L_s$ and $L_{sl}$ are the stator self-inductance and the stator leakage inductance, $L_r$ and $L_{rl}$ are the rotor self-inductance and the rotor leakage inductance, $\omega_{mr}$ is the angular speed of the rotor flux linkage vector, $\omega_r$ is the angular rotor speed, $J$ is the drive inertia, $f$ is the coefficient of viscose friction, $t_e$ and $t_l$ are the electrical and the load torque and $p$ is the number of pole pairs. From here on the steady-state quantities will be distinguished from the corresponding instantaneous values by capital letters.

In the induction motor model (1) magnetic saturation is introduced by variable inductance $L_m$, which is given by the nonlinear magnetizing curve $\Psi_m = f(i_m)$, where $\Psi_m$ and $i_m$ represent the magnetizing flux linkage and the magnetizing current.

## 3 Determination of the torque characteristics

The rotor flux linkage $\Psi_{rd}$ and the q-axis rotor current $i_{rq}$ in a steady-state are defined by equations (2) and (3).

$$\Psi_{rd} = L_r I_{rd} + L_m I_{sd} = L_m I_{sd} \tag{2}$$

$$\Psi_{rq} = L_r I_{rq} + L_m I_{sq} = 0 \;\Rightarrow\; I_{rq} = -\frac{L_m}{L_r} I_{sq} \tag{3}$$

The d-axis rotor current in steady-state $I_{rd}$ is expressed from the third equation in (1):

$$I_{rd} = -\frac{1}{R_r}\frac{d\Psi_{rd}}{dt} = 0 \tag{4}$$

Inserting (2) for the steady-state rotor flux linkage $\Psi_{rd}$ into the torque equation (1) yields:

$$T_e = p\frac{L_m^2}{L_r} I_{sd} I_{sq} \tag{5}$$

Rewriting the torque equation (5) to account for constant d-axis stator current $I_{sd}$, the corresponding torque characteristic $T_e = f(\frac{I_{sq}}{I_s})$ can be derived:

$$T_e = p\frac{L_m^2}{L_r} I_{sd} I_{sq} = p\frac{L_m^2}{L_r} I_{sd} I_s \left(\frac{I_{sq}}{I_s}\right) \tag{6}$$

Servo drives with the induction motor are usually operating with $I_{sd} = const.$ to guarantee good dynamic performance for all operating regimes. A set of torque characteristics for several constant d-axis stator currents $I_{sd}$, without and with consideration of magnetic saturation, are shown in Figs. 1 and 2, for the induction motor with the data given in appendix B.

It is obvious from Fig. 1 that the calculated torque without taking into account magnetic saturation is unusually high. Torque production when magnetic saturation is taken into account is reduced in Fig. 2, because of the reduction of mutual inductance value $L_m$ in (6), according to the magnetizing curve in Fig. 8.

The induction motor can operate with variable d-axis stator current $I_{sd}$, too. The allowed induction motor drive operation range is often limited by the stator current $I_s = \sqrt{I_{sd}^2 + I_{sq}^2}$. The torque characteristics of the controlled induction motor, calculated by equation (5) when $I_s = const.$, can be rewritten in the following form:

$$T_e = p\frac{L_m^2}{L_r} I_s^2 \sqrt{1 - \left(\frac{I_{sq}}{I_s}\right)^2}\left(\frac{I_{sq}}{I_s}\right) \tag{7}$$

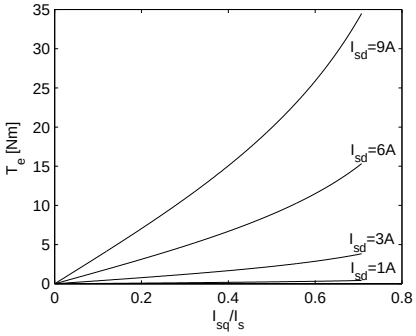


Figure 1. Torque characteristics for different $I_{sd}$ values (without magnetic saturation)

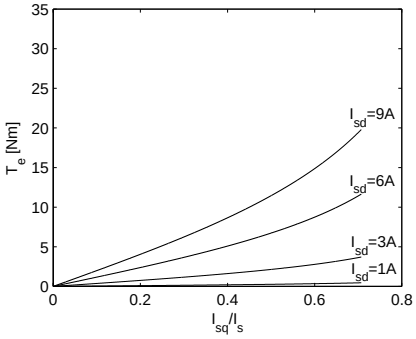


Figure 2. Torque characteristics for different $I_{sd}$ values (with magnetic saturation)

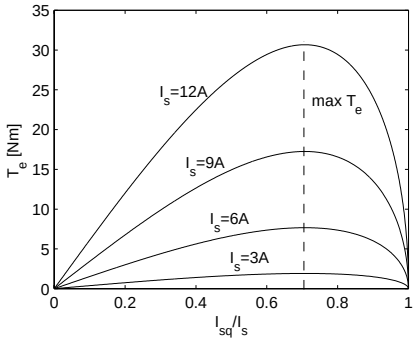


Figure 3. Torque characteristics for different $I_s$ values (without magnetic saturation)

Sets of the torque characteristics for several constant stator currents $I_s$, without and with consideration of magnetic saturation, are shown in Figs. 3 and 4 for the same induction motor.

The maximum value of the torque for a given value of $I_s$ can be obtained by taking the first derivative of the electromagnetic torque (7) with respect to the ratio $r = I_{sq}/I_s$ and by solving the maximum value of the ratio $r_{max}$ (equation 8).

$$\left(\frac{dT_e}{dr}\right) = 0 \quad \Rightarrow \; r_{max} \tag{8}$$

Neglecting magnetic saturation, (8) reduces to the following simple second order algebraic equation:

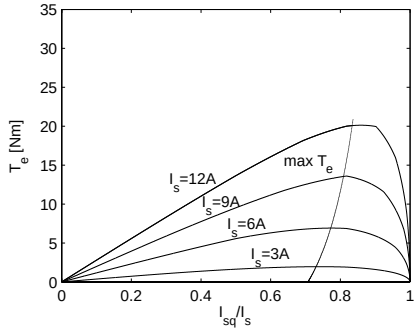


Figure 4. Torque characteristics for different $I_s$ values (with magnetic saturation)

$$2r_{max}^2 - 1 = 0 \tag{9}$$

with roots $r_{max1,2} = \pm\sqrt{2}/2$. This means that the maximal torque of the controlled induction motor drive is produced when $I_{sq}/I_s = 0,707$, i.e. $I_{sd} = I_{sq}$.

When (8) is solved, taking into account magnetic saturation, the following fourth order algebraic equation is obtained:

$$b_4 r_{max}^4 + b_2 r_{max}^2 + b_0 = 0 \tag{10}$$

where

$$\begin{aligned} b_4 &= -(2L_m - \tfrac{L_m^2}{L_r})(2L_m L_r - L_m^2)(L_m - L) - \\ &\quad -2\tfrac{L_m^2}{L_r}[-L_r(2L_m L_r - L_m^2) + \\ &\quad +(2L_m L_r - L_m^2 - L_r^2)(L_m - L)] \\ b_2 &= (2L_m - \tfrac{L_m^2}{L_r})(2L_m L_r - L_m^2)(L_m - L) + \\ &\quad +\tfrac{L_m^2}{L_r}[-L_r(2L_m L_r - L_m^2) + \\ &+ \quad (2L_m L_r - L_m^2 - L_r^2)(L_m - L)] - 2L_m^2 L_r^2 \\ b_0 &= L_m^2 L_r^2 \end{aligned} \tag{11}$$

Coefficients $b_4, b_2$ and $b_0$ are calculated in appendix A. The maximal torque curve is shown in Fig. 4 and is marked with $max\, T_e$. The maximal torque curve is drawn by changing the magnetizing current in the range $0 \le I_m \le I_{mmax}$ with the desired step. Using the nonlinear magnetizing curve given in Fig. 8, inductances $L_m, L$ and $L_r$ are calculated for the corresponding level of saturation. Then, equation (10) is solved for the root $r_{max}$ which satisfies $0 \le r_{max} \le 1$. For the corresponding value of magnetizing current $I_m$, the minimal steady-state stator current is obtained according to (17) by equation (12).

$$I_{smin} = \frac{I_m}{\sqrt{1 - \left(2\frac{L_m}{L_r} - \frac{L_m^2}{L_r^2}\right) r_{max}^2}} \tag{12}$$

The corresponding torque is calculated by using equation (7). The procedure is repeated for the whole range of the magnetizing current given in Fig. 8.

The described procedure, based on the relation (8), actually represents a mapping from the magnetizing curve $\Psi_m = f(I_m)$ (the domain with coordinates $\Psi_m, I_m$) to the torque characteristic $T_e = f(I_{sq}/I_s)$ (the domain with coordinates $T_e, I_{sq}/I_s$). It is obvious that the linear magnetizing curve with $L_m = const.$ is mapped to the vertical straight line $I_{sq}/I_s = \sqrt{2}/2$, while the actual nonlinear magnetizing curve $\Psi_m = f(I_m)$ is mapped to the mentioned $max\,T_e$ curve, which is obtained by inserting the roots $r_{max}$ ($0 \leq r \leq 1$) of algebraic equation (10) to the torque equation (7). The $max\ T_e$ curve in Fig. (4) starts at point $(I_{sq}/I_s)_0 = \sqrt{2}/2$.

Because of the shape of the torque characteristics shown in Fig. 4, the peak torque for a given value of stator current $I_s$ can be produced by the decreased value of the magnetizing current $I_{sd}$ indirectly, putting more stator current in the torque command current $I_{sq}$ [9].

In Fig. 5 the torque characteristics for three different values of $I_{sd} = const.$ and two torque characteristics for different values of maximal stator currents $I_{smax} = const.$, taking into account magnetic saturation, are given. The torque characteristics with $I_{smax} = const.$ limits the operating region of the induction motor drive, therefore the torque production loss $\Delta T$ is evident when an unsuitable value of the magnetizing reference current $I_{sd}$ is used.

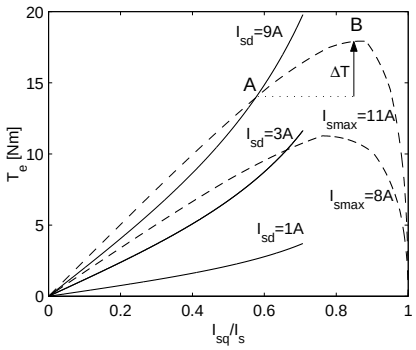


Figure 5. Torque characteristics for $I_{sd} = const.$ and corresponding current limitations $I_{smax}$

## 4 Magnetizing reference for achieving the steady-state peek torque-per-ampere ratio

The induction motor drives in RFOC usually operate with a high enough constant value of stator current $I_{sd}$ which guarantees excellent dynamic performances during the acceleration/deacceleration and load torque switching on. However, the steady-state stator current $I_s$ is frequently much higher than actually needed for the required load torque. The results from the previous section show that it is feasible and economically justified to use the torque characteristics at $I_s = const.$ with consideration of magnetic saturation to assure the peak torque per ampere ratio.

The maximal torque curve $maxT_e$ shown in Fig. 4 can be entered in a control algorithm in the form of a look-up table with the load torque $T_l$ as the input and the ratio $r_{max}$ as the output. For required load torque $T_l$, minimal stator current $I_{smin}$ is calculated according to (7) with equation (13).

$$I_{smin}^2 = T_l / \left[ p \frac{L_m^2}{L_r} \sqrt{1 - r_{max}^2}\, r_{max} \right] \tag{13}$$

The appropriate magnetizing stator current reference is given by equation (14),

$$I_{sd,ref} = \sqrt{I_{smin}^2 - I_{sq}^2} = I_{smin} \sqrt{1 - r_{max}^2} \tag{14}$$

which provides steady-state operation of the induction motor drive with a minimal stator current for the required load torque.

## 5 Experimental results

The maximal torque curve $max\ T_e$ was experimentaly determined for different load torque values. The RFOC algorithm was executed on the dSpace DS1103 microproccesor board. The rest of the equipment included: Semikron IGBT Voltage Source Inverter, Sever 3 kW induction motor with a wound rotor whose parameters are given in appendix B, and Mavilor Mo2000 DC motor with an Infranor DC power converter as the dynamic load.

At the beginning of each test the magnetizing current was set to $I_{sd,ref}$=9,3 A. After acceleration to 50 rad/s, the load torque with the value $T_l$=5 Nm, 7.5 Nm, 10 Nm, 12.5 Nm and 15 Nm was switched on. The stator current reference value $I_{sd,ref}$ was slowly reduced to reach the value of the minimal necessary stator current for the corresponding load torque, while the speed controller increased the current command $I_{sq}$ to compensate the reduced motor magnetization. The aim was to run the motor at a constant rotor speed in the domain where the motor torque is nearly equal to the load torque. The measured stator currents for the load torque $T_l$=10 Nm are shown in Fig. 6 and the best operation point is determined where $i_{s,min}$ is reached. Experimentally determined values of the ratio $I_{sq}/I_s$ are shown in Fig. 7 by the symbol *. The results of stator current reduction are shown in Table 1.

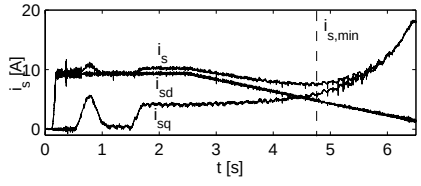


Figure 6. Diagram of stator currents $i_{sd}$, $i_{sq}$, $i_s$ during the test with $T_l$=10 Nm

As seen from Fig. 7, the test points are very close to the analytically calculated maximal torque curve $max\,T_e$,

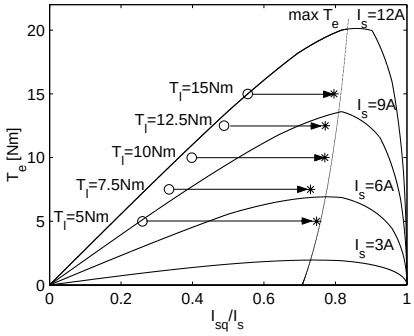


Figure 7. Torque characteristics, maximal torque curve and starting ($\circ$) and final ($*$) test points

thus confirming adequacy of the procedure proposed in sections 3 and 4 .

| $T_l$ (Nm) | 5 | 7.5 | 10 | 12.5 | 15 |
|---|---|---|---|---|---|
| before searching for minimal $I_s$ | | | | | |
| $I_{sd}(A)$ | 9.3 | 9.3 | 9.3 | 9.3 | 9.3 |
| $I_{sq}(A)$ | 2.5 | 3.3 | 4.2 | 5.2 | 6.2 |
| $I_s(A)$ | 9.63 | 9.87 | 10.56 | 10.65 | 11.18 |
| at the end of searching for minimal $I_s$ | | | | | |
| $I_{sd}(A)$ | 3.3 | 4.35 | 4.75 | 5.52 | 5.9 |
| $I_{sq}(A)$ | 3.7 | 4.6 | 5.7 | 6.65 | 7.76 |
| $I_{smin}(A)$ | 4.95 | 6.3 | 7.4 | 8.62 | 9.75 |

Table 1. Stator currents values while changing the reference of d-axis stator current $I_{sd}$

## 6 Conclusion

In this paper the steady-state torque characteristics of controlled induction motor at both $I_{sd} = const.$ and $I_s = const.$ are presented with and without taking into account magnetic saturation. A method for determination of the peak torque per ampere ratio curve with consideration of magnetic saturation is developed and experimentally proven. Application of the determined maximal torque curve in RFO induction motor control contributes significantly to the reduction of power losses under steady-state. However, for the reason of the lower magnetizing reference current, an inadequate dynamic performance could be expected in some applications.

## Appendix A

Equation (15) is obtained by derivating (7).

$$\begin{aligned}\tfrac{dT_e}{dr}\,|_{r_{max}} &= \tfrac{d}{dr}(p\tfrac{L_m^2}{L_r}I_s^2 r\sqrt{1-r^2})\,|_{r_{max}} = \\ &= pI_s^2[\tfrac{d}{dr}(\tfrac{L_m^2}{L_r})|_{r_{max}} r_{max}\sqrt{1-r_{max}^2}+ \\ &\quad +\tfrac{L_m^2}{L_r}(\tfrac{1-2r_{max}^2}{\sqrt{1-r_{max}^2}})] = 0\end{aligned} \tag{15}$$

Inductance derivative in (15) is caused by magnetic saturation given by the magnetization curve in Fig.(8).

The steady-state rotor currents $I_{rd}$ and $I_{rq}$ in RFOC ($\psi_{rq} = 0$) are:

$$\begin{aligned}I_{rd} &= -\tfrac{1}{R_r}\tfrac{d\Psi_{rd}}{dt} = 0 \\ I_{rq} &= -\tfrac{L_m}{L_r}I_{sq}\end{aligned} \tag{16}$$

The value of steady-state magnetizing current $I_m$ is according to (16) calculated by the equation (17).

$$\begin{aligned}I_m &= \sqrt{(I_{sd}+I_{rd})^2+(I_{sq}+I_{rq})^2} = \\ &= I_s\sqrt{1+(1-2\tfrac{L_m}{L_r}+\tfrac{L_m^2}{L_r^2}-1)(\tfrac{I_{sq}}{I_s})^2} = \\ &= I_s\sqrt{1-(2\tfrac{L_m}{L_r}-\tfrac{L_m^2}{L_r^2})r^2}\end{aligned} \tag{17}$$

Derivation of $L_m^2/L_r$ in (15) yields (18):

$$\frac{d}{dr}(\frac{L_m^2}{L_r}) = \frac{2L_m\frac{dL_m}{dr}L_r - \frac{dL_r}{dr}L_m^2}{L_r^2} = (2\frac{L_m}{L_r}-\frac{L_m^2}{L_r^2})\frac{dL_m}{dr} \tag{18}$$

because:

$$L_r = L_{rl}+L_m \;\Rightarrow\; \frac{dL_r}{dr} = \frac{dL_m}{dr} \tag{19}$$

Derivation of the mutual inductance $L_m$ with respect to the ratio $r$ yields the equation (20):

$$\begin{aligned}\tfrac{dL_m}{dr} &= \tfrac{dL_m}{dI_m}\tfrac{dI_m}{dr} = \tfrac{d}{dI_m}(\tfrac{\Psi_m}{I_m})\tfrac{dI_m}{dr} = \\ &= \tfrac{\frac{d\Psi_m}{dI_m}I_m-\Psi_m}{I_m^2}\tfrac{dI_m}{dr} = -\tfrac{L_m-L}{I_m}\tfrac{dI_m}{dr}\end{aligned} \tag{20}$$

Derivation of $I_m$ with respect to the $r$, according to (17), yields (21).

$$\begin{aligned}\tfrac{dI_m}{dr} &= I_s\tfrac{1}{2\sqrt{1-(2\frac{L_m}{L_r}-\frac{L_m^2}{L_r^2})r^2}}\tfrac{d}{dr}[1-(2\tfrac{L_m}{L_r}-\tfrac{L_m^2}{L_r^2})r^2] = \\ &= I_s^2\tfrac{1}{2I_m}[-\tfrac{d}{dr}(2\tfrac{L_m}{L_r}-\tfrac{L_m^2}{L_r^2})r^2 - 2r(2\tfrac{L_m}{L_r}-\tfrac{L_m^2}{L_r^2})] = \\ &= \tfrac{I_s^2}{I_m}[\tfrac{2L_mL_r-L_m^2-L_r^2}{L_r^3}\tfrac{dL_m}{dr}r^2 - r\tfrac{2L_mL_r-L_m^2}{L_r^2}]\end{aligned} \tag{21}$$

Equation (21) is inserted in (20) and equation (22) is obtained.

$$\begin{aligned}\tfrac{dL_m}{dr} &= -\tfrac{L_m-L}{I_m}\tfrac{I_s^2}{I_m}\Big[\tfrac{2L_mL_r-L_m^2-L_r^2}{L_r^3}\tfrac{dL_m}{dr}r^2 - \\ &\quad -\tfrac{2L_mL_r-L_m^2}{L_r^2}r\Big]\end{aligned} \tag{22}$$

From equation (22) $dL_m/dr$ is expressed as :

$$\begin{aligned}&\Big[1+\tfrac{2L_mL_r-L_m^2-L_r^2}{L_r^3}(L_m-L)\tfrac{I_s^2}{I_m^2}r^2\Big]\tfrac{dL_m}{dr} = \\ &= \tfrac{2L_mL_r-L_m^2}{L_r^2}(L_m-L)\tfrac{I_s^2}{I_m^2}r\end{aligned} \tag{23}$$

i.e.:

$$\frac{dL_m}{dr} = \frac{\frac{2L_mL_r-L_m^2}{L_r^2}(L_m-L)\frac{I_s^2}{I_m^2}r}{1+\frac{2L_mL_r-L_m^2-L_r^2}{L_r^3}(L_m-L)\frac{I_s^2}{I_m^2}r^2} \tag{24}$$

The ratio $I_s^2/I_m^2$ is determined from (17):

$$\frac{I_s^2}{I_m^2} = \frac{1}{1-(2\frac{L_m}{L_r}-\frac{L_m^2}{L_r^2})r^2} = \frac{L_r^2}{L_r^2-(2L_mL_r-L_m^2)r^2} \tag{25}$$

and inserted in (24) to obtain:

$$\begin{aligned}\frac{dL_m}{dr} &= [L_r(2L_mL_r - L_m^2)(L_m - L)r]/ \\ &\{L_r^3 + [-(2L_mL_r - L_m^2)L_r + \\ &+(2L_mL_r - L_m^2 - L_r^2)(L_m - L)]r^2\}\end{aligned} \quad (26)$$

The equation (15) obtains the following form:

$$\begin{aligned}&(2\frac{L_m}{L_r} - \frac{L_m^2}{L_r^2})(\frac{dL_m}{dr})|_{r_{max}} r_{max}\sqrt{1 - r_{max}^2} + \\ &+\frac{L_m^2}{L_r}\frac{1-2r_{max}^2}{\sqrt{1-r_{max}^2}} = 0\end{aligned} \quad (27)$$

where $(\frac{dL_m}{dr})_{r_{max}}$ is defined by (26).
The ratio $r_{max} = I_{sq}/I_s$ is solution of the fourth-order algebraic equation (28).

$$\begin{aligned}&-\{(2L_m - \frac{L_m^2}{L_r})(2L_mL_r - L_m^2)(L_m - L) + \\ &+2\frac{L_m^2}{L_r}[-L_r(2L_mL_r - L_m^2) + \\ &+(2L_mL_r - L_m^2 - L_r^2)(L_m - L)]\}r_{max}^4 + \\ &+\{(2L_m - \frac{L_m^2}{L_r})(2L_mL_r - L_m^2)(L_m - L) + \\ &+\frac{L_m^2}{L_r}[-L_r(2L_mL_r - L_m^2) + \\ &+(2L_mL_r - L_m^2 - L_r^2)(L_m - L)] - 2L_m^2L_r^2\}r_{max}^2 + \\ &+L_m^2L_r^2 = 0\end{aligned} \quad (28)$$

## Appendix B

Parameters of the 3 kW induction motor with the wound rotor Sever ZPD112MK4:

$$\begin{array}{rclrcl} R_s &=& 1.976\ \Omega & R_r &=& 2.91\ \Omega \\ L_m &=& 0.223\ \text{H} & & & \\ L_s &=& 0.2335\ \text{H} & L_r &=& 0.2335\ \text{H} \\ J &=& 0.031\ \text{kgm}^2 & & & \\ f &=& 0.0007\ \text{Nms/rad} & & & \\ T_n &=& 15\ \text{Nm} & & & \end{array}$$

The magnetizing curve is shown in Fig .8.

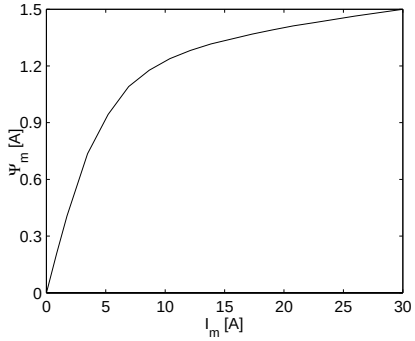


Figure 8. Magnetizing curve

## 7 References


[1] P. Vas, *Electrical machines and drives: a space-vector theory approach*, Oxford University press, Oxford, 1992.

[2] E. Levi, "A unified approach to main flux saturation modelling in d-q axis models of induction machines", *IEEE Trans. on Energy Conversion*, Vol. 10, No. 3, pp. 455-461, 1995.

[3] J. O. Ojo, A. Consoli, T. A. Lipo, "An improved model of saturated induction machines", *IEEE Transactions on Industry Applications*, Vol. 26, No. 2, pp. 212-220, March/April 1990.

[4] J. C. Moreira, T. A. Lipo, "Modelling of saturated ac machines including air gap flux harmonic components", *IEEE Transactions on Industry Applications*, Vol. 28, No. 2, pp. 343-349, September 1997.

[5] E. Levi, S. Vukosavić, V. Vučković, "Saturation compensation schemes for vector controlled induction motor drives", *PESC'90 Record*, pp. 591-598, 1990.

[6] P. Vas, *Sensorless vector and direct torque control*, Oxford University press, Oxford, 1998.

[7] E. Levi, M. Sokola, S. N. Vukosavić, "A method for magnetizing curve identification in rotor flux oriented induction machines", *IEEE Transactions on Energy conversion*, Vol. 15, No. 2, pp. 157-162, June 2000.

[8] F. M. H. Khater, R. D. Lorenz, D. W. Novotny, K. Tang, "Selection of flux level in field-oriented induction machine controllers with consideration of magnetic saturation effects", *IEEE Trans. on Industry Applications*, Vol. 23, No. 2, pp. 276-281, March/April 1987.

[9] R. D. Lorenz, D. W. Novotny, "Saturation effects in field-oriented induction machines", *IEEE Trans. on Industry Applications*, Vol. 26, No. 5, pp. 283-289, March/April 1990.

[10] I. T. Wallace, D. W. Novotny, R. D. Lorenz, D. M. Divan, "Increasing the dynamic torque per ampere capability of induction machines", *IEEE Trans. on Industry Applications*, Vol. 30, No. 1, pp. 146-153, January/February 1994.

[11] R. T. Novotnak, J. Chiasson, M. Bodson, "High-performance motion control of an induction motor with magnetic saturation", *IEEE Trans. on Control Systems Technology*, Vol. 7, No. 3, pp. 315-327, 1999.

[12] J.-K. Seok, S.-K. Sul, "Optimal flux selection of an induction machine for torque maximization", *IEEE International Electric Machines and Drives Conference*, Milwaukee, WI, USA, pp. TB3-2, 1997.

[13] A. Baba, E. Mendes, A. Razek, "Losses minimisation of a field-oriented controlled induction machine by flux optimisation accounting for magnetic saturation", *IEEE International Electric Machines and Drives Conference*, Milwaukee, WI, USA, pp. MD1-2, 1997.



**Petar Ljušev** received his B.S.E.E. degree from the "Sts. Cyril and Methodius" University, Skopje, Macedonia in 2000 and his M.Sc. degree from the University of Maribor, Maribor, Slovenia in 2002. He is currently with the Technical University of Denmark, Copenhagen, working towards his Ph.D. degree. He has worked on modelling and control design of the induction motor taking into account magnetic saturation. His research interests include power electronics, modelling and control syntheses of electromechanical systems.

**Drago Dolinar** received his B.S.E.E., M.Sc. and Ph.D. degrees in electrical engineering from the University of Maribor, Maribor, Slovenia in 1978, 1980 and 1985, respectively. Since 1981 he has been with the Faculty of Electrical Engineering and Computer Science of the University of Maribor where he is Professor at present. His current research interests include modelling and control of electrical machines.

**Gorazd Štumberger** received his B.S.E.E., M.Sc. and Ph.D. degrees in electrical engineering from the University of Maribor, Slovenia in 1989, 1992 and 1996, respectively. Since 1989 he has been with the Faculty of Electrical Engineering and Computer Science of the University of Maribor. His current research interests include modelling and control of electrical machines.